International Journal of Heat and Mass Transfer 122 (2018) 1–10

Contents lists available at ScienceDirect

International Journal of Heat and Mass Transfer

journal homepage: www.elsevier.com/locate/ijhmt

Thermal conductivity of highly porous metal foams: Experimental and image based finite element analysis

Yasin Amani [a], Atsushi Takahashi [b], Patrice Chantrenne [a,*], Shigenao Maruyama [c], Sylvain Dancette [a], Eric Maire [a]

[a] INSA de Lyon, MATEIS CNRS UMR5510, Université de Lyon, 69621 Villeurbanne, France
[b] Graduate School of Engineering, Tohoku University, 6-6, Aoba, Aramaki, Aoba-ku, Sendai, Miyagi 980-8579, Japan
[c] Institute of Fluid Science, Tohoku University, 2-1-1, Katahira, Aoba-ku, Sendai, Miyagi 980-8577, Japan

ARTICLE INFO

Article history:
Received 2 August 2017
Received in revised form 11 January 2018
Accepted 13 January 2018

Keywords:
Image analysis
3-D modeling
Numerical simulation
Measurement
Open-cell foam
Conduction

ABSTRACT

X-ray tomography is used to produce three-dimensional images of an aluminium alloy foam with a high porosity (> 93%). These data allow describing the foam structure from which a finite element model is derived to predict the thermal conductivity of the foam. The results are compared with experimental values measured by a new guarded hot plate apparatus adapted for the range of thermal conductivity values of interest. Good agreement is observed which validated the finite element model used to evaluate the thermal properties of any porous metallic foam with stochastic cell size and configuration. Furthermore, the thermal conductivity of the foam has also been predicted using previous analytical models. The differences with previous values show that it is important to account for the real geometry of the foam to get an accurate value of the thermal conductivity.

1. Introduction

Manufacturing technologies produce new types of porous materials which are widely used as key elements where low Thermal Conductivity (TC) is required. Therefore, they are mostly applied for refrigeration [1], thermal energy storage [2] and insulation [3] purposes. They divide into closed-cell and open-cell types based on their morphologies. For each cell type, the structure might be stochastic or periodic. Open-cell foams normally have higher TC than closed-cell foams of similar densities due to bigger cell sizes and disclosed gas volume which causes convection [4].

In the case of open-cell foams, the architecture and material of the foam skeleton influence TC. Bhattacharya et al. [5] mentioned that the value of TC depends strongly on the foam porosity and the configuration of struts and their intersections. Afterwards, Singh and Kasana [6] stated that TC relies on the ratio of the TC of the constituents as well. Peak et al. [7] mentioned that TC increases as the porosity decreases. However, it varies little by changing the cell size at fixed porosity.

Heat transfer mechanism through a foam is a consequence of conduction in the solid phase, conduction and convection in the gaseous phase and thermal radiation. The contribution of each heat transfer mechanism is a key factor when the TC is supposed to be set to a desired value while keeping the porosity fixed. Calmidi and Mahajan [8] remarked that at low temperatures, (between 333 and 348 K) nonlinear effects such as natural convection and radiation are negligible. However, at higher temperatures, they have a significant influence on TC [9–13]. In this paper, we focus on the prediction of the solid phase contribution to TC. The studied foam is a 40 PPI (Pores Per Inch) Duocel® open-cell foam produced by ERG Aerospace Corporation depicted in Fig. 1. The samples are made of 6101 aluminium alloy subjected to a T6 precipitation-hardening heat treatment. The prediction and measurements are done in two conditions: first the foam with air and secondly the foam embedded in epoxy resin. The densities and TC of aluminium, air and epoxy resin are given in Table 1. These parameters do not vary significantly within the temperature ranges considered in this study. Thus, they are assumed to be constant. For the first configuration, it has been shown that the convective and radiative heat transfer are negligible as compared to conduction heat transfer. For the second configuration, the convective and radiative heat transfers are suppressed. So, the experimental and predicted values might be directly compared.

The geometry of the foam is determined using X-ray tomography (Section 2). The measurement methodology is

* Corresponding author.
E-mail address: patrice.chantrenne@insa-lyon.fr (P. Chantrenne).

https://doi.org/10.1016/j.ijheatmasstransfer.2018.01.050
0017-9310/

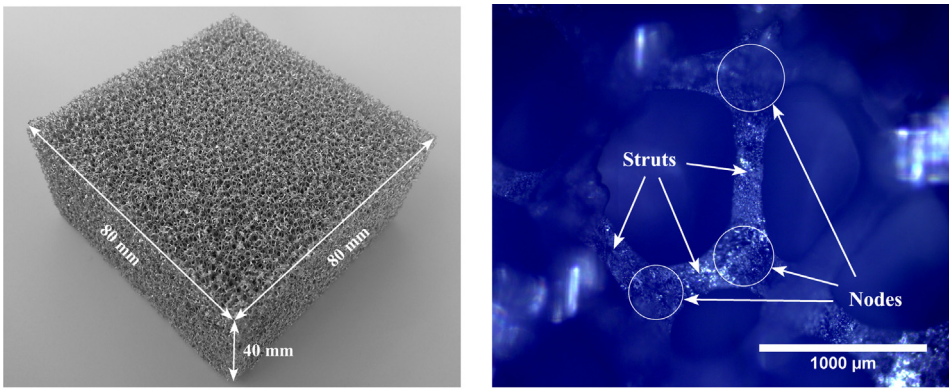

Fig. 1. (a) Open-cell aluminium alloy foam with a porosity of $\varepsilon = 0.927$. (b) Close-up view of a single cell of the foam via optical microscopy.

Table 1
TC and densities of foam components.

Material	Density ($kg{\cdot}m^{-3}$)	TC ($W \cdot m^{-1} \cdot K^{-1}$)
6101-T6	2700 [14]	218 [15]
Epoxy resin	1147	0.1813
Air (305 K, 1 atm)	1.1839	0.0265

detailed in Section 3. From the geometry obtained by X-ray tomography, a Finite Element (FE) analysis is conducted to predict the conduction part of TC (Section 4). Also, the X-ray tomography images are used to extract the geometrical characteristics to evaluate the conduction part of TC using analytical models (Section 5). The results are compared in the last section.

2. Tomography

The architecture of the foam block is obtained by X-ray tomography [16,17]. It relies on the Beer-Lambert law which implies that every line integral of the attenuation coefficient along the X-ray beam path corresponds to an object in the recorded projection [18]. The result is a Two-Dimensional (2-D) image of a Three-Dimensional (3-D) object projected on the detector screen. In order to obtain the 3-D structure, the sample is rotated in 720 steps between 0° and 360° and an average of three images is taken at each step. Then, a standard filtered back-projection algorithm is used to reconstruct the final 3-D image.

The best resolution that can be obtained by global tomography depends on the dimensions of the sample and the size of the detector. Several tricks are played to scan the whole samples that are 80 mm × 80 mm × 40 mm. The distance between the detector and the X-ray tube shown in Fig. 2(a) is fixed. The sample can be displaced in x direction and the closer to the X-ray tube results in the better resolution obtained by the detector. In a common tomography procedure, the detector is fixed in front of the X-ray tube and the sample should be placed at distance x_1 away from the detector. However the resolution obtained using this technique is 46 µm, which is not enough in this study. Therefore, another method called "double detector" or "stitching" tomography is used. In this method, the detector is displaced in the y direction which expands the cone beam volume recorded. The sample can then be placed at distance x_2, closer to the X-ray tube, which provides a 23 µm resolution. Also, the sample is displaced in the z direction to be scanned locally step by step as illustrated in Fig. 2(b). The X-ray tube operates at an acceleration voltage of 80 kV using a tungsten transmission target with a 280 µA current. The spot size is between 2–3 µm during all scans.

Nodes and struts of the foam are analysed in the 3-D image using the Fiji software to evaluate node-to-node distance and average node and strut thicknesses (Table 3). In order to evaluate node-to-node distance distribution, voxels from the edges of the solid phase in the binary 3-D image are removed using the Binary-Erode plugin of Fiji. Voxels of struts are removed entirely while some voxels of nodes remain by repeating the erosion procedure because the average node thickness is higher than that of the struts. The clusters of voxels are labelled by giving them different colours. An in-house plugin is used to compute node-to-node distances. This plugin computes all minimum distances between pairs of labelled objects.

The solid phase is analysed using the local thickness plugin of Fiji. The plugin estimates the local thickness by the largest sphere that fits in the solid phase and contains its voxels. The result of the analysis is a 3-D stack of the foam structure with different colours corresponding to different local thicknesses. The histogram plot of colours in such 3-D image illustrating the number of voxels against local thickness has two peaks, the average strut diameter and the average node diameter respectively.

Table 2
Dimensions of the samples used in this study.

Sample no.	Configuration	Width (mm)	Length (mm)	Depth (mm)
1	Foam-air	79.79 ± 0.39	79.91 ± 0.43	09.75 ± 0.44
2	Foam-air	79.93 ± 0.18	79.94 ± 0.24	20.03 ± 0.19
3	Foam-air	80.03 ± 0.09	80.15 ± 0.31	30.00 ± 0.18
4	Foam-air	79.79 ± 0.95	79.89 ± 0.85	39.98 ± 0.44
5	Foam-resin	79.88 ± 0.33	79.97 ± 0.49	09.36 ± 0.10
6	Foam-resin	79.21 ± 0.35	79.42 ± 0.51	19.05 ± 0.10
7	Foam-resin	79.37 ± 0.62	79.49 ± 0.25	29.33 ± 0.16
8	Foam-resin	78.91 ± 0.33	79.06 ± 0.06	39.32 ± 0.11